Available online at www.sciencedirect.com
SCIENCE DIRECT®
Polymer Degradation and Stability 82 (2003) 441–450
Polymer Degradation and Stability
www.elsevier.com/locate/polydegstab

# Nanocomposites based on poly (ϵ-caprolactone) (PCL)/clay hybrid: polystyrene, high impact polystyrene, ABS, polypropylene and polyethylene

Xiaoxia Zheng, Charles A. Wilkie*

*Department of Chemistry, Marquette University, PO Box 1881, Milwaukee, WI 53233, USA*

Received 26 April 2003; accepted 16 May 2003

**Abstract**

Nanocomposites of polystyrene, high impact polystyrene, acrylonitrile–butadiene–styrene terploymer, polypropylene and polyethylene have been prepared using an organically-modified clay that contains polycaprolactone—PCL-modified clay. Depending upon the mode of preparation of the PCL-modified clay, all three types of nanocomposites, immiscible, intercalated and exfoliated, may be produced. The materials have been characterized by X-ray diffraction, transmission electron microscopy, cone calorimetry, thermogravimetric analysis, and the evaluation of mechanical properties.


*Keywords:* Nanocomposite; Polycaprolactone; Polyoletins; Styrenics

## 1. Introduction

Polymer clay nanocomposites exhibit many unique properties, including increased heat distortion temperature, reduced flammability and simultaneously improved physical properties of the polymer, which make these materials very attractive. The preparation of a nanocomposite can be accomplished either by a blending process or by polymerization. The type of nanocomposite that is obtained, immiscible, intercalated or exfoliated, is ordinarily quite dependent upon the preparative process that is used [1].

The most commonly used clay for polymer/clay nanocomposites is montmorillonite (MMT), which has an inorganic ion balancing the charge in the gallery space of the clay. This clay must be modified in order to make it organophilic enough so that it can interact with the typical organic polymer. This is usually accomplished by ion-exchanging the inorganic cation with an ammonium, or other 'onium' ion, that contains at least one long alkyl chain.

It is well-known that one can easily obtain exfoliated nanocomposites of polycaprolactone both by melt blending this polymer with a clay or by an in situ polymerization of ϵ-caprolactone in the presence of the clay. Poly (ϵ-caprolactone) may form hydrogen bonds with the hydroxy groups on the clay surface and it also exhibits compatibility with a great variety of other polymers [2]. Thus one may expect that the presence of polycaprolactone within the gallery space may permit one to form nanocomposites of other polymers.

Nanocomposites of polycaprolactone have been widely reported [3–12]. These have been prepared both by blending and by ring opening polymerization of ϵ-caprolactone. The preparation of exfoliated materials is easier for this polymer than for many other polymers. Two of the papers cited above are especially germane to the work herein described [6,12]. In these papers PCL has essentially been used as a compatibilizer to enable the formation of an exfoliated nanocomposite with a polymer for which the formation is otherwise difficult; in one case polyurethane and in the other styrene–acrylonitrile (SAN) copolymer.

In this study, poly(ϵ-caprolactone) (PCL) clay nanocomposites are prepared either by melt blending of PCL with organically-modified clay or by in situ ring opening polymerization of ϵ-caprolactone (CL) with organically-

* Corresponding author. Tel.: +1-414-288-7065; fax: +1-414-288-7066.
*E-mail address:* charles.wilkie@marquette.edu (C.A. Wilkie).

0141-3910/03/$ - see front matter © 2003 Elsevier Ltd. All rights reserved.
doi:10.1016/S0141-3910(03)00197-6

modified clay. This new organically-modified clay was then melt blended with polystyrene (PS), high impact polystyrene (HIPS), acrylonitrile–butadiene–styrene terpolymer (ABS), polypropylene (PP) and polyethylene (PE) to give nanocomposites.

## 2. Experimental

### 2.1. Materials

Most chemicals used in this study, including poly(ϵ-caprolactone) ($M_w = 65{,}000$, $T_m = 60$ °C), ϵ-caprolactone (99%, bp = 98–99 °C/2 mmHg), PS (Melt flow index 200 °C/5 kg, 7.5 g/10 min, $M_w = 230{,}000$), PE (low density, Melt flow index, 190 °C/2.16 kg, 7 g/10 min), PP (Isotactic, Melt flow index, 230 °C/2.16 kg, 0.5 g/10 min) were acquired from Aldrich Chemical Co. ABS (Magnum 275, 230 °C/3.8 kg, 2.6 g/10 min) and HIPS (Melt flow index 200 °C/5 kg, 6 g/10 min) were provided by the Dow Chemical Company. Methyl tallow bis-2-hydroxyethyl ammonium modified clay, Cloisite 30B and dimethyl dehydrogenated tallow alkyl ammonium modified clay, Cloisite 15A, were provided by Southern Clay Products, Inc.

### 2.2. Instrumentation

Thermogravimetric analysis (TGA) was performed on a Cahn TG-131 instrument under a flowing nitrogen atmosphere at a scan rate of 10 °C/min from 20 to 600 °C; temperatures are reproducible to ±3 °C, while the error bars on the fraction of nonvolatile material is ±3%. Cone calorimetry was performed using an Atlas Cone 2 instrument according ASTM E 1354-92 at an incident flux of 35 kW/m$^2$ or 50 kW/m$^2$ using a cone shaped heater. Exhaust flow was set at 24 l/s and the spark was continuous until the sample ignited. Cone samples were prepared by compression molding the sample (20–50 g) into square plaques using a heated press. Typical results from Cone calorimetry are reproducible to within about ±10%. These uncertainties are based on many runs in which thousands of samples have been combusted [13,14]. X-ray diffraction was performed on a Rigaku Geiger Flex, 2-circle powder diffractometer; scans were take from 2 theta 0.86 to 10, step size 0.1, and scan time per step of 10 s. Bright field transmission electron microscopy (TEM) images of the composites were obtained at 60 kV with a Zeiss 10c electron microscope. The samples were ultramicrotomed with a diamond knife on a Riechert-Jung Ultra-Cut E microtome at room temperature to give ~70 nm thick sections. The sections were transferred from the knife-edge to 600 hexagonal mesh Cu grids. The contrast between the layered silicates and the polymer phase was sufficient for imaging, so no heavy metal staining of sections prior to imaging is required. Mechanical properties were obtained using a Reliance RT/5 (MTS System Corporation, Model NO 4501029) computerized system for material testing at a crosshead speed of 0.2 in/min and 5 kN load cell. The samples were prepared both by injection molding, using an Atlas model CS 183MMX minimax molder, and by stamping from a sheet; the reported values are the average of six determinations.

### 2.3. Preparation of PCL/clay by in situ polymerisation [6]

A 90 g sample of ϵ-caprolactone (dried over $CaH_2$ and distilled under reduced pressure prior to use) and 10 g of 30B were combined in a three neck flask and stirred at room temperature for 4 h, then heated to 170 °C and maintained at this temperature for 48 h. After cooling, the resulting solid was dispersed in THF and then precipitated by the addition of hexane and dried in vacuo. In order to determine if any polymer had become attached to the clay, the new organically-modified clay was extracted with acetone overnight and the fraction that was recovered was compared to the amount of clay that was originally present. When 10% 30B clay was used, the residue after extraction had a mass of 21–27%; between 10 and 20% of the mass of polymer was attached to the clay.

### 2.4. Preparation of PCL/clay by melt blending

A sample of clay (pre-dried at 80 °C for 12 h) and PCL were initially dry-mixed in a beaker, typically using 10% clay. This was then melt blended in a Brabender Plasticorder, which was equipped with 50 cm$^3$ cell, at high speed (60 rmp) at 100 °C for 30 min. The material was removed from the mixer and permitted to cool to room temperature. It was then again charged to the Brabender and blended at 90 °C for 20 min.

### 2.5. Preparation of polymer–clay nanocomposites

All the nanocomposites prepared in this study were melt blended in a Brabender Plasticorder at high speed (60 rmp) at 190 °C for 15 min for the PS, HIPS, ABS, PP and PE. The composition of each nanocomposite is calculated from the amount of organic clay and polymer charged to the Brabender. The typical ratio is 70% polymer and 30% PCL/clay, which corresponds to 3% clay in the final system. The material code used shows first of all the clay used, 30B or 15A, then the way in which the polycaprolactone clay was obtained, either CL for the monomer or PCL for the polymer. In all cases the polycaprolactone clay was prepared using 10% clay and the nanocomposite contained 70% polymer and 30% organically-modified clay; this corresponds to 3% clay in all systems.

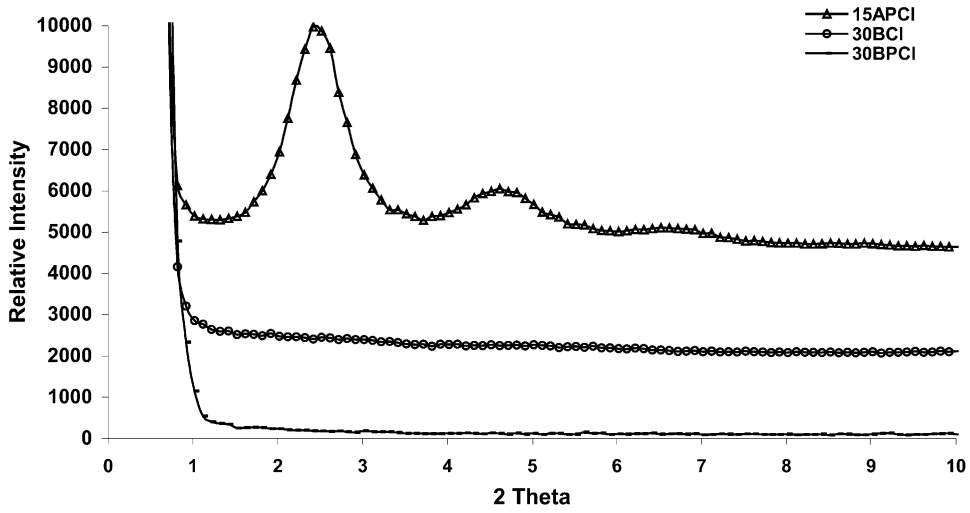


Fig. 1. XRD patterns of PCL/clay.

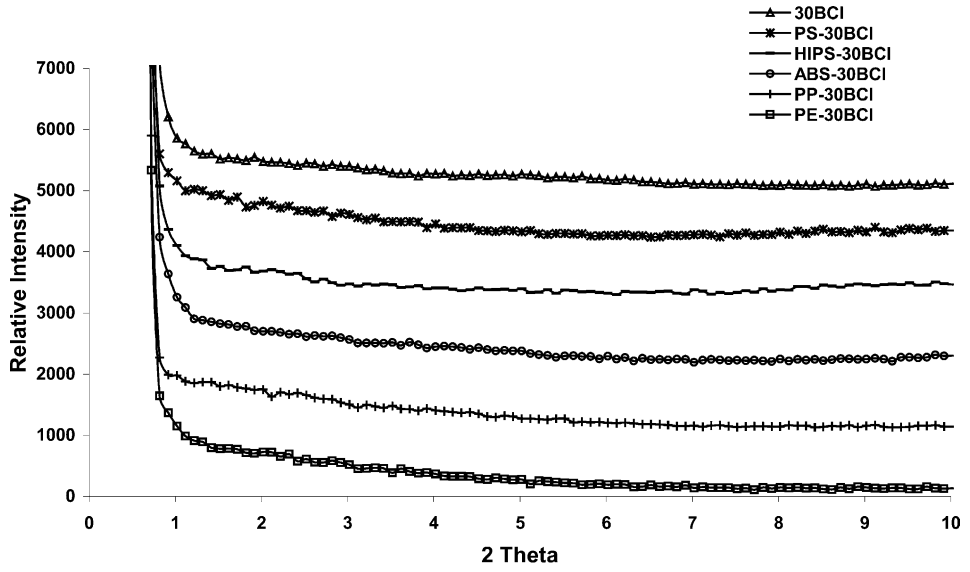


Fig. 2. XRD patterns of polymer/30BCL nanocomposites.

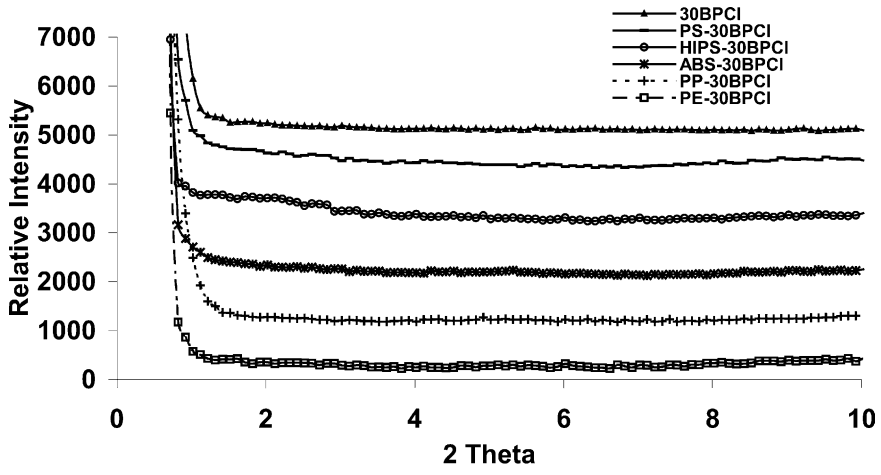


Fig. 3. XRD patterns of polymer/30BPCL nanocomposites.

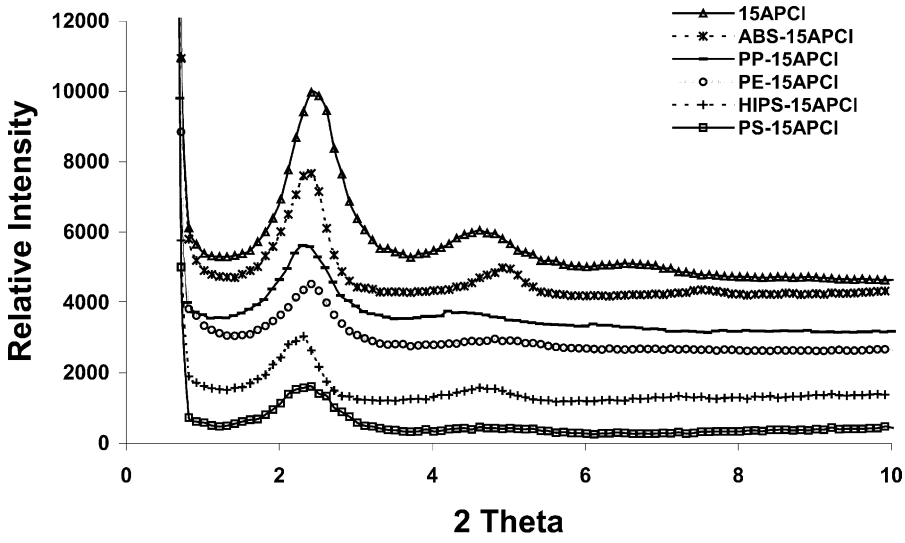


Fig. 4. XRD patterns of polymer/15APCL nanocomposites.

### 2.6. Measurement of molecular weight

The PCL/clay masterbatches, which were prepared via in situ polymerization, were extracted with refluxing acetone reflux for 48 h, then the molecular weights were determined by intrinsic viscosity measurements using the relation $[\eta] = 9.94 \times 10^{-5}\ Mw^{0.82}$ in benzene at 30 °C [15]. The viscosity average molecular weight of the extracted PCL was $15{,}000 \pm 5000$. $T_m = 60$–$70$ °C.

## 3. Results and discussion

Two new organically-modified clays were prepared in this study by either melt blending polycaprolactone (PCL) with a clay or by doing a ring-opening polymerization of ϵ-caprolactone in the presence of a clay. One of the clays that was used, 15A, contains no functionality, i.e., it simply contains alkyl moieties and organically-modified clays were prepared only by melt blending with PCL. The other clay, 30B, contains hydroxyl groups which could react with the oligomer as it forms. New organically-modified clays were prepared both by melt blending and by polymerization. When the amount of clay used was 10%, it was determined that there was between 20 and 30% insoluble material so a relatively large fraction of material did attach to the clay, presumably by reaction with the OH groups.

### 3.1. XRD measurement of PCL/clay

There is a big difference between the organically-modified clay that is prepared using the non-functionalized 15A clay and the clay which has hydroxyl functionalities attached to it, as shown by the XRD traces that are seen in Fig. 1. For the 15A clay, peaks are apparent while there are no peaks for the 30B clay, regardless of whether it was prepared by melt blending or by in situ polymerization. Fig. 2 shows the XRD traces for the nanocomposites that were prepared using the in situ organically-modified 30B clay while Fig. 3 shows the analogous traces for the melt blended 30B system. Five different polymers, polystyrene (PS), high impact polystyrene (HIPS), acrylonitrile–butadiene–styrene terpolymer (ABS), polypropylene (PP) and polyethylene (PE), have been studied and no peaks are seen for all polymers. This would normally indicate either that an exfoliated nanocomposite had been produced or that there was sufficient disorder introduced by the preparation process so that peaks cannot be seen. In the case of the 15A clay, peaks are seen for each polymer, as shown in Fig. 4. The *d*-spacing is a little smaller for each of these nanocomposites than it is for the clay, but the change is quite small. Based only on the XRD traces, one must suggest that the nanocomposites formed with

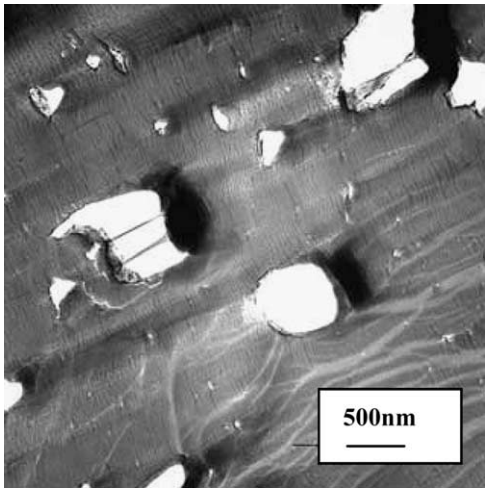


Fig. 5. TEM images for PS-30BPCL nanocomposites at low magnification.

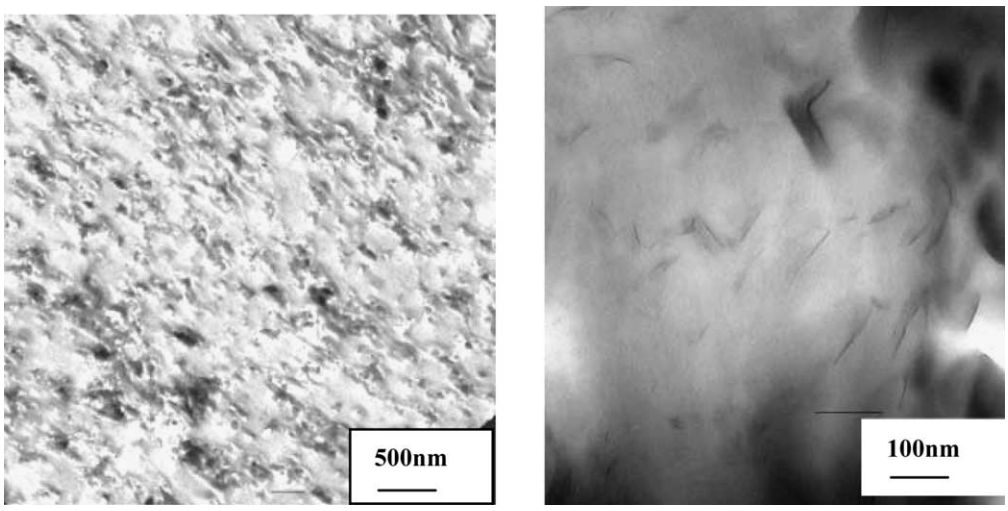


Fig. 6. TEM images for ABS-30BPCL nanocomposites at low (left) and high (right) magnification.

the 30B clay are likely to be exfoliated while those formed from 15A clay are intercalated.

### 3.2. Transmission electron microscopy

One may not rely only on XRD results to ascertain the type of nanocomposite that has been formed, some other technique is also required. The usual technique that is used is transmission electron microscopy, TEM, but other techniques, including cone calorimetry may be used. TEM images have been obtained at both low and high magnification for all of the systems that have been studied and the images are presented in Figs. 5–8. There are miscibility problems associated with the combination of PCL with some of these polymers and this is reflected in the TEM images, as a consequence in some cases only images obtained at low magnification are presented while in other cases those at high magnification, which show the exfoliated nature of the nanocomposites, are shown. Fig. 5 shows the low magnification image of the PS nanocomposite. Clay layers are not visible in this but one can clearly see the domains of PCL and PS [9]. Fig. 6 shows the images at both low and high magnification for the ABS nanocomposite. At low magnification, one can see the PCL domains but one can also see the clay layers. At high magnification, the individual clay layers are distinctly visible and it is clear that an exfoliated system has been produced. The low magnification image of the PE nanocomposite is shown in Fig. 7. Again, miscibility is an issue and the clay is not visible. On the other hand, Fig. 8 presents the high magnification image of the PP nanocomposite and again the individual clay layers and the exfoliated nature of the nanocomposite is clearly seen.

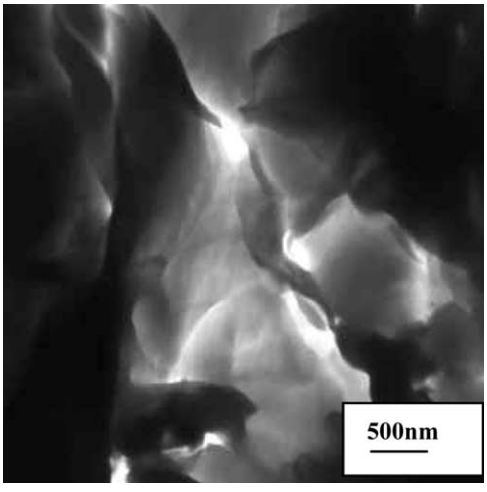


Fig. 7. TEM images for PE-30BPCL nanocomposites at low magnification.

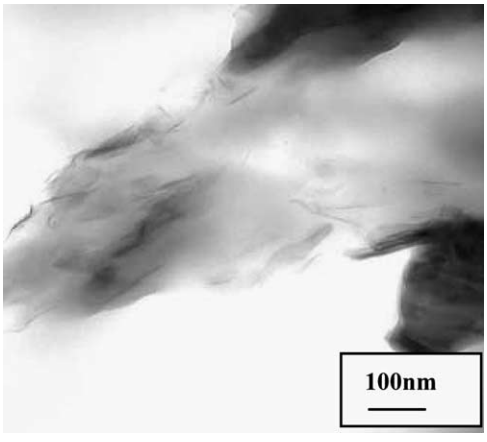


Fig. 8. TEM images for PP-30BPCL nanocomposites at high magnification.

Table 1
TGA results for PCl/clay and its nanocomposites

| Sample | $T_{10\%}$ (°C) | $T_{50\%}$ (°C) | Char (%) |
|---|---|---|---|
| 30BCl | 387 | 408 | 11 |
| 14APCl | 395 | 419 | 11 |
| 30BPCl | 386 | 416 | 10 |
| PS | 370 | 422 | 0 |
| PS-30BCl | 391 | 447 | 8 |
| PS-15APCl | 407 | 449 | 2 |
| PS-30BPCl | 395 | 451 | 4 |
| HIPS | 414 | 442 | 2 |
| HIPS-30BCl | 394 | 459 | 6 |
| HIPS-15APCl | 410 | 454 | 2 |
| HIPS-30BPCl | 411 | 461 | 5 |
| ABS | 402 | 431 | 3 |
| ABS-30BCl | 418 | 450 | 7 |
| ABS-15APCl | 419 | 447 | 5 |
| ABS-30BPCl | 424 | 455 | 4 |
| PP | 354 | 431 | 1 |
| PP-30BCl | 394 | 470 | 6 |
| PP-15APCl | 415 | 473 | 2 |
| PP-30BPCl | 404 | 479 | 5 |
| PE | 398 | 469 | 1 |
| PE-30BCl | 393 | 499 | 5 |
| PE-15APCl | 412 | 493 | 2 |
| PE-30BPCl | 401 | 504 | 4 |

### 3.3. TGA characterization of nanocomposites

The thermal stability of the nanocomposites has been examined by thermogravimetric analysis (TGA); the information that seems to be most important to characterize thermal stability is the onset temperature of the degradation, which is measured both by the temperature at which 10% degradation occurs ($T_{10\%}$) and the mid-point of the degradation ($T_{50\%}$), and the fraction which is not volatile at 600 °C, denoted as char. The data for all of the nanocomposites is shown in Table 1 and the TGA curves are shown in Figs. 9–14. The first comments should be on the clays themselves; these clays show very good thermal stability, with 10% degradation occurring around 390 °C. This is significantly higher than what is observed for the starting materials, 15A shows 10% degradation at 330 °C while the value for 30B is 320 °C. The clays alone undergo degradation in two steps, a Hofmann elimination, giving a trialkylammonium cation, followed by the loss of the amine leaving only a proton as the counterion. The enhanced thermal stability in the presence of PCL must indicate this degradation is inhibited. There is very little temperature difference between 10 and 50% degradation, which shows the steepness of the degradation curve. In general, the temperatures of both 10 and 50% degradation are enhanced for the nanocomposites relative to the virgin polymers. There is apparently a greater enhancement for the clays prepared by melt blending of the polymer than for that prepared by in situ polymerization. This is likely due to the higher molecular weight for the polymer as compared to the in situ polymerized material. In previous work from this laboratory, a clay which contains a styrene oligomer was prepared [16]. The enhancements in the onset temperature are larger for this PCL modified clay than for the styrene-modified clay.

The TGA curves for both PP and PE nanocomposites show two steps in the degradation, while the virgin polymers show only a single step. The onset temperature is greatly enhanced for these systems; it appears that the PCLpresent in the clay must undergo the initial degradation and this must stabilize the PP and PE so that they will degrade at higher temperature. No explanation for these observations is currently available.

### 3.4. Cone calorimetric characterization of nanocomposites

In previous work from this laboratory and other groups, it has been shown that nanocomposites have enhanced fire retardancy [13,14,16]. The suggested mechanism is that an aluminosilicate layer is built up on

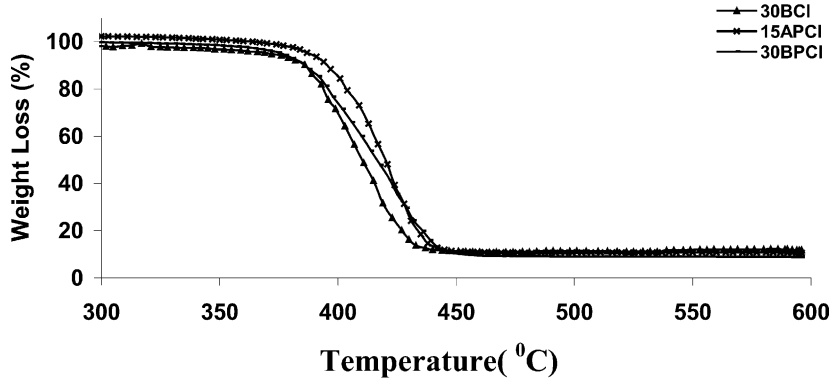


Fig. 9. TGA curve of PCL/clay hybrids.

the surface during burning, which may act as a barrier to both mass transport of degrading polymer to the vapor phase and to insulate the polymer from the flame. Cone calorimetry is usually used to evaluate the fire properties of polymers; the parameters that are available include: the time to ignition, the heat release rate curve, the specific extinction area, SEA, a measure of smoke, and the mass loss rate. The normal observation for nanocomposites is that the time to ignition is normally decreased, i.e. the nanocomposites are actually easier to ignite than are the virgin polymer; the peak heat release rate is decreased, the% reduction is very polymer dependent; the total heat released is similar for the virgin polymer and nanocomposites, which means that all of the polymer will burn; the smoke increases by a small amount; and the mass loss rate is decreased. The results are shown in Table 2. The reduction in peak heat release rate (PHRR) must be compared with previous

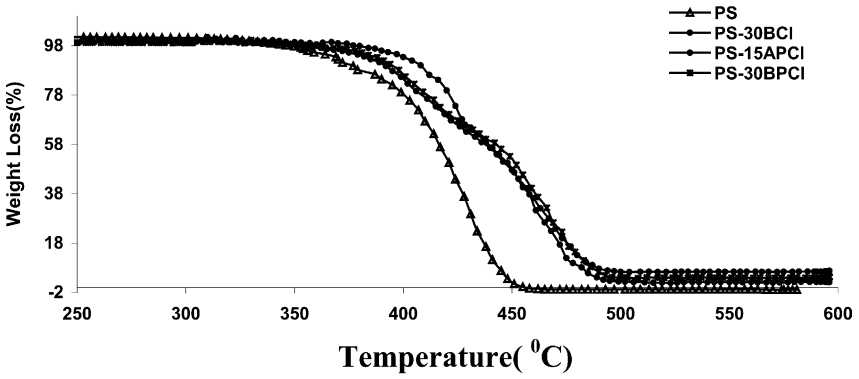


Fig. 10. TGA curve of PS-PCL/clay nanocomposites.

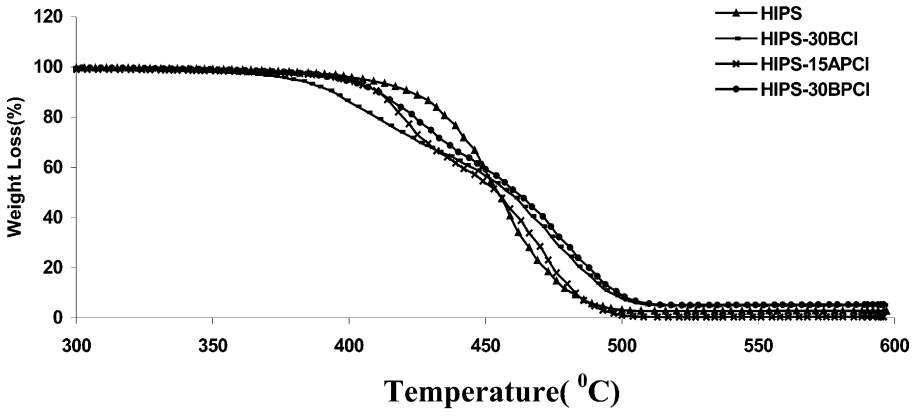


Fig. 11. TGA curve of HIPS-PCL/clay nanocomposites.

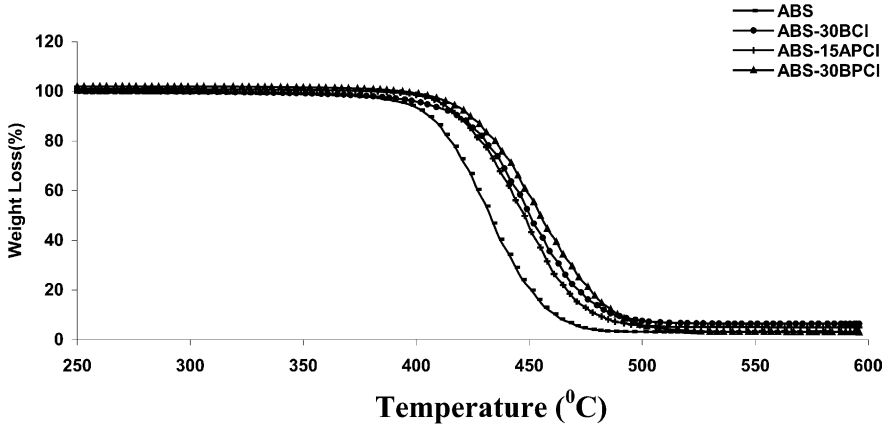


Fig. 12. TGA curve of ABS-PCL/clay nanocomposites.

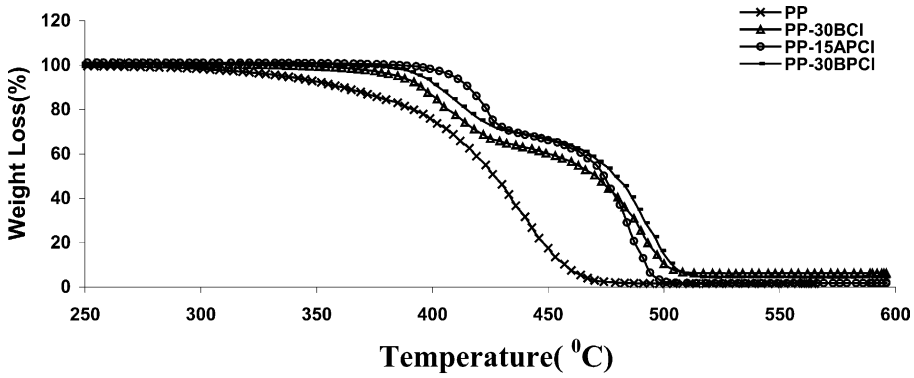


Fig. 13. TGA curve of PP-PCL/clay nanocomposites.

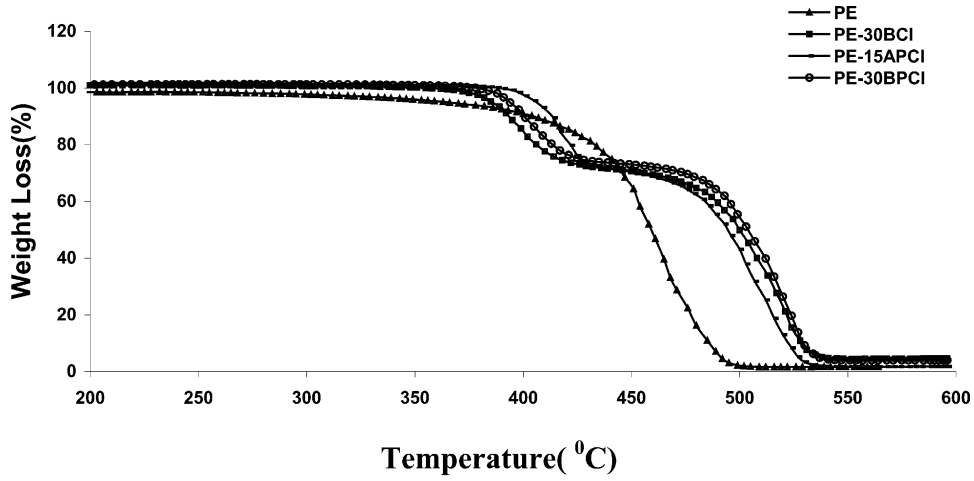


Fig. 14. TGA curve of PE-PCL/clay nanocomposites.

Table 2
Cone data of PCl/clay nanocomposites at 35 kW/m$^2$

| Sample | Time to ignition (s) | PHRR[a], kW/m$^2$ (% reduction)[b] | Time top PHRR (s) | Total heat released (MJ/m$^2$) | SEA[c] (m$^2$/kg) | Mass loss rate (g/s.m$^2$) |
|---|---|---|---|---|---|---|
| PS | 53±7 | 1425±178 | 113±4 | 89±2 | 980±28 | 35±2 |
| PS-30BCl | 47±4 | 735±34 (48%) | 117±9 | 79±3 | 1203±56 | 21±1 |
| PS-15APCl | 50±4 | 832±38 (42%) | 77±2 | 84±3 | 1233±37 | 22±1 |
| PS-30BPCl | 46±1 | 483±8 (66%) | 79±6 | 78±2 | 1280±12 | 13±1 |
| HIPS | 60±6 | 1348±11 | 99±1 | 93±3 | 1051±69 | 32±1 |
| HIPS-30BCl | 47±1 | 854±4 (36%) | 105±5 | 85±3 | 1211±7 | 24±0 |
| HIPS-15APCl | 61±4 | 929±16 (31%) | 120±19 | 86±5 | 1197±21 | 25±1 |
| HIPS-30BPC1 | 69±1 | 569±1 (58%) | 114±1 | 80±2 | 1286±24 | 16±1 |
| ABS | 57±3 | 1146±35 | 116±2 | 92±2 | 944±7 | 27±0 |
| ABS-30BCl | 71±1 | 1114±41 (3%) | 120±3 | 90±0 | 1201±1 | 29±1 |
| ABS-15APCl | 71±2 | 1241±45 (0%) | 110±3 | 92±0 | 1093±11 | 30±0 |
| ABS-30BPC1 | 67±3 | 831±94 (27%) | 117±9 | 77±8 | 1070±2 | 24±2 |
| PP | 55±3 | 1733±179 | 119±4 | 109±3 | 541±26 | 24±1 |
| PP-30BCl | 40±6 | 850±78 (51%) | 84±1 | 91±3 | 627±29 | 17±2 |
| PP-15APCl | 52±2 | 1565±136 (11%) | 122±8 | 122±5 | 657±11 | 23±1 |
| PP-30BPC1 | 49±4 | 704±8 (59%) | 115±4 | 94±0 | 710±15 | 15±1 |
| PE | 76±3 | 1740±37 | 134±6 | 114±6 | 533±32 | 22±1 |
| PE-30BCl | 75±0 | 1156±106 (34%) | 119±6 | 107±7 | 667±9 | 18±1 |
| PE-15APCl | 79±2 | 1484±102 (15%) | 165±4 | 98±1 | 531±8 | 23±1 |
| PE-30BPC1 | 71±2 | 861±21 (51%) | 102±12 | 92±1 | 579±22 | 15±1 |

[a] PHRR, peak heat release rate
[b] (% reduction), [PHRR (virgin polymer) - PHRR (nanocomposite)]/PHRR
[c] SEA, Specific Extinction Area

values for the various polymers in order to evaluate these reductions. The reduction expected for PS is about 60%, for HIPS, about 40%, for ABS, about 25%, for PP, about 35% and for PE, about 30%. A reduction of less than 15% should be taken as a indication that nanocomposite formation has not occurred. Thus all three organically-modified clays give nanocomposite formation for PS and HIPS. The difference between the polymerized and the melt blended clays may be attributed to the difference in molecular weights of the materials used. The reduction in PHRR for HIPS is larger than any that have been previously reported. For ABS, no nanocomposite is formed with the in situ organically-modified clay nor for the 15A clay. Likewise nanocomposites are not formed for PP and PE with the 15A clay. The reductions observed for both PP and PE are larger than values that have been previously reported. The times to ignition are perhaps a little longer than have been previously observed and the total heat released is almost the same as that of the virgin polymer, indicating that all of the polymer does eventually burn. These values are about what would expect for nanocomposite formation.

### 3.5. Evaluation of mechanical properties

All the mechanical properties, including Young's modulus, stress at break, strain at break of all nanocomposites and virgin polymers, are reported in Table 3. The variation in Young's modulus is not consistent for all of the polymers. For PP and PE, the in situ polymerized material gives the largest value while this gives the lowest Young's modulus for PS, HIPS and ABS. Since this material has the lowest molecular weight for the clay, one may expect the results observed for the styrenics, but not for the polyolefins. No explanation can be offered at this time to explain the variation in mechanical properties.

Table 3
Mechanical properties of PCL/clay nanocomposites

| Sample | Stress at break (Mpa) | Strain at break (%) | Modulus (Gpa) |
|---|---|---|---|
| PS | 34.4±7.4 | 1.62±0.28 | 4.06±0.30 |
| PS-30BCl | 17.4±2.5 | 0.82±0.16 | 3.97±0.48 |
| PS-15APCl | 31.4±4.9 | 1.21±0.20 | 4.09±0.30 |
| PS-30BPCl | 41.2±7.2 | 1.21±0.15 | 4.97±0.34 |
| HIPS | 17.5±1.2 | 2.40±1.80 | 2.87±0.09 |
| HIPS-30BCl | 12.4±1.5 | 0.80±0.06 | 2.55±0.23 |
| HIPS-15APCl | 21.2±2.0 | 1.06±0.10 | 2.69±0.14 |
| HIPS-30BPCl | 19.7±1.7 | 0.84±0.07 | 3.03±0.14 |
| ABS | 26.8±1.7 | 11.78±6.13 | 2.58±0.04 |
| ABS-30BCl | 17.9±0.3 | 11.16±0.36 | 1.54±0.17 |
| ABS-15APCl | 21.5±0.8 | 30.03±10.53 | 2.01±0.10 |
| ABS-30BPCl | 20.4±0.5 | 55.68±7.52 | 1.92±0.11 |
| PP | 30.5±2.1 | 3.07±0.52 | 2.53±0.20 |
| PP-30BCl | 13.8±4.7 | 1.42±0.49 | 2.59±0.32 |
| PP-15APCl | 23.1±2.8 | 3.39±1.24 | 2.30±0.37 |
| PP-30BPCl | 23.0±3.3 | 2.45±0.68 | 2.69±0.39 |
| PE | 9.0±0.8 | 41.05±6.02 | 0.31±0.04 |
| PE-30BCl | 7.9±0.9 | 8.41±2.73 | 0.86±0.10 |
| PE-15APCl | 11.5±1.0 | 46.01±10.96 | 0.75±0.15 |
| PE-30BPCl | 11.9±1.1 | 67.73±10.21 | 0.56±0.03 |

## 4. Conclusions

Polymer/clay nanocomposites of polystyrene, HIPS, ABS, PP and PE can be the prepared by blending with organically-modified clays that contain polycaprolactone. The PCL is essentially serving as a compatibilizer to enhance the compatibility between the polymer and the clay. Exfoliated nanocomposites result when a clay which contains hydroxyl functionality is used while either immiscible or intercalated nanocomposites are formed when the starting clay does not contain functional groups on the ammonium cation. Most nanocomposites of polypropylene are produced using PP-g-MA as a compatibilizer while, in this system, virgin polypropylene may be used. The starting clay and the mode by which the PCL is added to the clay has a large effect on the type of material that is produced. The reduction in peak heat release rate is larger, for some polymers, than has been previously observed. Cone calorimetry is a useful technique to probe nanocomposite formation.

## Acknowledgements

This work was performed under the sponsorship of the US Department of Commence, National Institute of Standards and Technology, Grant Number 70NANB6D0119. We thank Peggy Miller, University of Texas Health Center in San Antonio, and Ben Knesek, Southern Clay Products, obtaining the transmission electron micrographs.

## References

[1] Wang D, Zhu J, Yao Q, Wilkie CA. Chem Mater 2002;14:3837–43.
[2] Heuschen J, Jerome R, Teyssie P. J Polym Sci: Polym Phys Ed 1989;27:523–44.
[3] Messersmith PB, Gianellis EP. Chem Mater 1993;5:1064–6.
[4] Messersmith PB, Gianellsi EP. J Polym Sci: Polym Chem 1995; 33:1047–57.
[5] Jimenez G, Ogata N, Kawai H, Ogihara T. J Appl Polym Sci 1997;64:2211–20.
[6] Chen TK, Tien YI, Wei KH. J Polym Sci: Polym Chem 1999; 37:2225–33.

[7] Kubies D, Pantoustier N, Dubois P, Rulmont A, Jerome R. Macromol 2002;35:3318–20.
[8] Lepoittevin B, Pantoustier N, Devalckenaere M, Alexandre M, Kubies D, Calberg C, Jerome R, Dubois P. Macromol 2002; 35:8385–90.
[9] Pantoustier N, Lepoittevin B, Alexandre M, Keubies D, Calberg C, Jerome R, Dubois P. Polym Eng Sci 2002;42:1928–37.
[10] Lepoittevin B, Devalckenaere M, Pantoustier N, Alexandre M, Kubies D, Calberg C, Jerome R, Dubois P. Polymer 2002; 43:4017–23.
[11] Gorrasi G, Tortora M, Vittoria V, Galli G, Chiellini E. J Polym Sci: Part B: Polym Phys 2002;40:1118–24.
[12] Kim SW, Jo WH, Lee MS, Ko MB, Jho JY. Polymer 2001; 42:9837–42.
[13] Gilman JW, Kashiwagi T, Nyden M, Brown JET, Jackson CL, Lomakin S, Giannelis EP, Manias E. In: Al-Malaika S, Golovoy A, Wilkie CA, editors. Chemistry and technology of polymer additives. Blackwell Scientific; 1999. p. 249–65.
[14] Gilman JW, Kashiwagi T, Giannelis EP, Manias E, Lomakin S, Lichtenham JD, Jones P. In: Le Bras M, Camino G, Bourbigot S, Delobel R, editors. Fire retardancy of polymeric materials, the use of intumescence, Royal Society of Chemistry, Cambridge, pp. 203–21.
[15] Hao J, Yuan M, Deng X. J Appl Polym Sci 2002;86:676–83.
[16] Su S, Wilkie CA, submitted.